American Journal of Clinical and Experimental Medicine
2023; 11(3): 52-57
http://www.sciencepublishinggroup.com/j/ajcem
doi: 10.11648/j.ajcem.20231103.12
ISSN: 2330-8125 (Print); ISSN: 2330-8133 (Online)

Diagnostic Value of Simple Pulmonary Apex Pleural Hypertrophy and Adhered (sPAPHA) in Chest CT Examination of Young People (18-40 Years)

He Xinhua[1], Cao Hetao[2, *]

[1]Department of Medical Imaging, People's Hospital of Rugao, Rugao, China

[2]Department of Medical Imaging, Affiliated Hospital of Nantong University, Nantong, China

Email address:

hexinhua9999@sina.com (He Xinhua), caohetao321@126.com (Cao Hetao)

[*]Corresponding autho

To cite this article:

He Xinhua, Cao Hetao. Diagnostic Value of Simple Pulmonary Apex Pleural Hypertrophy and Adhered (sPAPHA) in Chest CT Examination of Young People (18-40 Years). *American Journal of Clinical and Experimental Medicine.* Vol. 11, No. 3, 2023, pp. 52-57.
doi: 10.11648/j.ajcem.20231103.12

Received: May 4, 2023; **Accepted**: May 25, 2023; **Published**: June 6, 2023

Abstract: *Objective* To explore the rationality of Simple Pulmonary Apex Pleural Hypertrophy and Adhered (sPAPHA) in Multi-slice Computed Tomography (MSCT) chest examination of young people (18 – 40 years). *Materials and methods* Of the 6710 pieces of the chest MSCT data collected from healthy subjects aged 18 to 40 years, 152 were diagnosed with sPAPHA and were divided into two groups (group A and B). Among them, 51 cases showing radiologic pleuroparenchymal fibroelastosis (radio-PPFE) were classified as group A, the remaining 101 cases group B. The image of lung apex, the inclination angle of the median rib (IAR), the anteroposterior to transverse diameter ratio (R) and the shape of cupula pleurae were compared between the two groups. 37 cases of spontaneous pneumothorax were also taken into consideration to observe the pleural cavity adhesions attached to the rough surface. *Results* The diagnostic rate of sPAPHA was 2.27% and radio-PPFE was 0.76%, accounting for 33.55% of sPAPHA. The pleural thickness of lung apex was 4.69±2.56 mm in group A, greater than 2.86±1.47 mm in group B; the displayed rate of apex line was 76.47% in group A, higher than 3.96% in group B; the size of IAR was (51.42±7.23) in group A, smaller than (59.25±9.37) in group B; the R value was 2.89±1.65 in group A, greater than 2.21±1.02 in group B; and the proportions of arc type and depressed pleural apices were 21.57% and 78.43% in group A, 88.12% and 11.88% in group B. The differences above were of statistical significance ($P<0.05$). In 37 cases of spontaneous pneumothorax, there were 74 cases of inflated pleural cavity on the rough pleural surface with striated shadow, and 7 cases of pleural cavity adhesion (9.46%). *Conclusion* The diagnosis of early mild PPFE may be reasonable, as sPAPHA partially presents as radio-PPFE and has flat chest features. Rough pleural surfaces with pleural cavity at the striated shadow could not be used as evidence for the diagnosis of pleural adhesion.

Keywords: Pulmonary Apex, Flat thorax, Pleura, MSCT

1. Introduction

The diagnosis of Pulmonary Apex Pleural Hypertrophy and Adhered (PAPHA) is commonly reported in chest examination with Multi-slice Computed Tomography (MSCT), even among the young population (aged 18 to 40 years). Since these young people have no other significant chest abnormalities, neither clinical symptoms nor specific medical history, we refer to it as simple PAPHA (sPAPHA). What is the relationship between pulmonary apical cap (PAC), radiologic pleuroparenchymal fibroelastosis (radio-PPFE) and sPAPHA? In this paper, we counted 6,710 cases of chest MSCT data from 2018-2020 in healthy check-ups aged 18 to 40 years in People's Hospital of Rugao and Affiliated Hospital of Nantong University through the picture archiving and communication system (PACS), and analyzed 152 of them with the diagnosis of PAPHA, aiming to improve the awareness and diagnostic rationality of this disease.

2. Materials and Methods

2.1. General Materials

There were 65 males and 87 females with an average age of 28.26±8.51 years of the 152 cases diagnosed with sPAPHA. Among them, 51 cases showing radio-PPFE were set up as group A, while the remaining 101 cases were set up as group B. 37 cases of spontaneous pneumothorax were also collected to observe the pleural cavity adhesions attached to the rough surface. Diagnostic criteria of sPAPHA: in addition to PAPHA, only ground glass opacity (GGO), tracheobronchial diverticula (TBD), a few fibrotic lesions outside the superior lobe of lung, calcification, a small range of chronic inflammation and a few mild bronchiectasis or isolated bullae of lung outside the upper lobe can be regarded as one of the combined symptoms.

2.2. Inspection and Measurement of MSCT

MSCT plain scan was performed on Siemens Somatom Definition AS+, Philips Brillance 64 and Philips Brilliance 256 iCT, with a layer thickness of 5 mm or 6 mm, pitch 1, and collimation 0.625-0.750 mm. Scan parameters: 120-140 kV, 120 mA, FOV: 30 or 35 cm. Using real-time multiplanar reconstruction (MPR), the apex of the apical lung was obtained in coronal or sagittal position by moving the reconstructed centerline up to the point where the inflated lung tissue disappeared, and sagittal position through the highest point of the apical lung was obtained by moving the reconstructed centerline to this point. A horizontal tangent was made through this point and the lower edge of the first posterior rib, and the distance between the two lines was measured as the maximum thickness of the apical pleura.

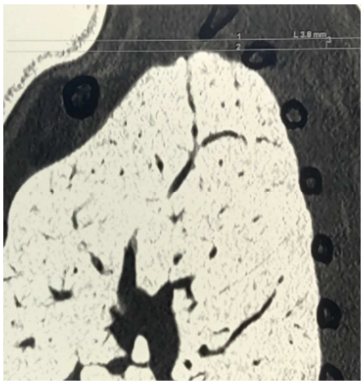

Figure 1. *Male, 28 years old, sPAPHA The maximum thickness: 3.3mm, the lower margin of PAC is smooth and slightly irregular.*

The left-right and anterior-posterior diameters of the thorax were measured at the level of tracheal carina, then we calculated the anteroposterior to transverse diameter ratio (R). In the 3D reconstructed side image of the thoracic ribs, the line between the midpoint of the posterior superior border and the midpoint of the anterior inferior border of the sixth rib, forms the inclination angle of the median rib (IAR) with the coronal plane [1].

2.3. Symptom Evaluation

A tilted coronal reorganization along the mid-tracheal axis was performed to observe the morphology of the cupula pleurae, which was roughly divided into two categories: the circular arc type, whose top axillary of the pleura has a circular-shaped lateral edge, and the depressed type, whose lateral edge of the cupula pleurae axilla was partially collapsed.

Figure 2. *Male, 31 years old, sPAPHA The cupula pleurae is medially inclined, with naturally smooth curvature of the first, second and third axillary ribs.*

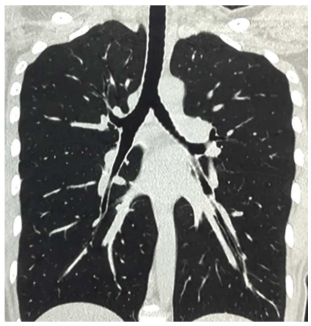

Figure 3. *Male, 35 years old, radio-PPFE The cupula pleurae is depressed, the first rib relative to the second and third rib reverse arc collapse-like change.*

Using the 1 mm thin layer technique at the top of the lung apex, a dense septal line surrounding the bulla-like structure in the lung is shown as the pulmonary apex line (PAL).

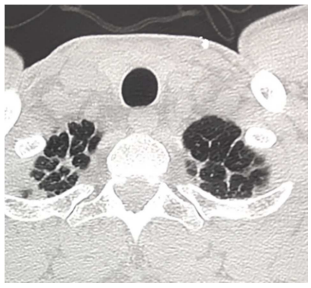

Figure 4. *Male, 27 years old, radio-PPFE The cross section of the lung apex showed signs of pseudobulla surrounding the PAL.*

Bilateral pleural hypertrophy in the upper lungs with multiple subpleural triangular cone shaped solid shadows with the tip pointing to the hilum or with radio-PPFE extending around the apex of the lung were classified as group A [2].

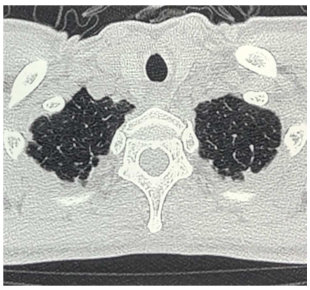

Figure 5. *Male, 29 years old, radio-PPFE The cross section clearly showed thickening of soft tissue in the pleura and subpleura on both sides of the lung apex, and multiple inverted triangular high-density shadows in the lower rough margin.*

Figure 6. *Male, 37 years old, radio-PPFE The coronal view clearly showed thickening of soft tissue in the pleura and subpleura on both sides of the upper lung. The lower margin was rough with multiple small triangles and shoe-nail shaped high-density shadows pointing to the hilum of the lung.*

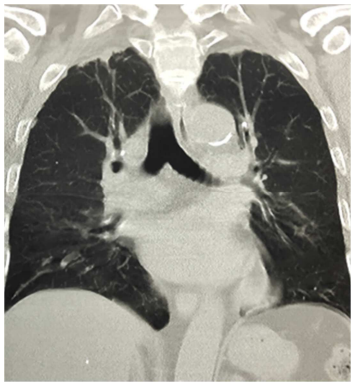

Figure 7. *Male, 45 years old, radio-PPFE The coronal view clearly showed thickening of two superior pleura. The lower pleura margin was rough and presented with multiple short triangular dense shadow. The apical (posterior) segment of bronchus was pulled.*

Cases with pleural hypertrophy limited to the apex of the lung with few or no subpleural triangular solid shadows and unilateral pleural hypertrophy were classified as group B. (Figure 1).

Counting methods of rough and irregular pleural surface with high-density shadow of varying lengths protruding into the lung: discontinuous independent counting in cross-section at the same level, discontinuous independent counting in cross-section at the upper and lower levels, and not counting in areas not affected by pneumothorax. All images were observed and judged independently by two experienced senior physicians, and unified by consultation in case of disagreement.

2.4. Statistics Processing

SPSS 20.0 statistical software was applied for data analysis. Kappa consistency test was performed for image observation, and $k<0.4$ was considered as poor consistency, $0.4\leq k<0.75$ as fair consistency, and $k\geq 0.75$ as good consistency. The measurement data were expressed as $\chi\pm s$, and the t-test was used to compare the differences between groups, and the count data were expressed as frequency and rate, and the χ^2 test was used to compare the differences between groups. The difference was considered statistically significant at $P<0.05$.

3. Results

3.1. Conformity Test

Two senior physicians independently observed consistent K-values of radio-PPFE of 0.87, PAL of 0.79, the cupula pleurae morphology judgment of 0.82, sPAPHA thickness of 0.80, IAR size of 0.78, and R-value measurement of 0.79, all with K-values greater than 0.75, thus all of which were good.

3.2. MSCT Performance

Group A: Transverse views showed irregular hypertrophy of soft tissues at the anterior inner edge of the first and second posterior axillary ribs, and the inner edge of the thickened soft tissues was serrated, studded or island-shaped, all of which were bilateral. (Figure 4) Pleural hypertrophy was obvious at the apical part of the lung in the upper posterior part, and disappeared at the lower level to the dorsal part of the lower lobe. The thickening phenomenon was basically absent at the anterior ribs and costal cartilage. 39 cases (76.47%) and 71 sides (69.51%) showed PAL, and 55 sides (53.92%) showed signs of pseudobulla surrounded by PAL at one or more levels. (Figure 4) The MPR showed a crescent-shaped soft tissue shadow in coronal and sagittal view, with the lower edge curved on four sides, forming a thicker, longer, inverted triangular, inverted pyramidal or shoe nail-shaped high-density shadow perpendicular to the pleural margin. (Figure 5) 37 sides (36.27%) bronchovascular bundle in posterior segment of superior leaf tip was slightly tracted. (Figure 6) Sagittal 84 sides (82.35%) had pleural thickness greater than 5 mm.

Figure 8. *Male, 23 years old, radio-PPFE The lower margin of the sagittal PAC was irregularly serrated, pointing to the hilum of the lung. The thickness of the lung pleura was 6.8mm.*

Group B: the cross section showed a thin layer of soft tissue at the inner edge of the ribs with a smooth inner edge, serial cross section from cephalad → pedicle, from circumferential → "C" shape → metaphyseal, mainly located in the lateral posterior side. 4 cases (3.96%) and 5 sides (2.48%) showed PAL, whose incidence was significantly lower than that of group A, and the difference was statistically significant (χ^2=19.26, P<0.01). The coronal and sagittal views showed a crescent-shaped soft tissue shadow, with mostly smooth lower margins and a few slightly rough, forming a small number of thin, short, nearly perpendicular to the margins, high-density strip shadow with pleural thickness less than 5 mm. (Figure 1).

3.3. Comparison of Clinical and Imaging Findings

Of the 6710 physical examiners (aged 18- 40 years), the diagnostic rate of sPAPHA was 152 cases (2.27%) and radio-PPFE was 51 cases (0.76%), accounting for 33.55% of sPAPHA. The sPAPHA thickness and R-value in group A were greater than those of group B, while and the IAR was smaller than that of group B. See Table 1. Shape of cupula pleurae: 40 cases (78.43%) of depressed type and 11 cases (21.57%) of circular arc type in group A; 12 cases (11.88%) of depressed type and 89 cases (88.12%) of rounded type in group B. The cupula pleurae was mainly depressed type in group A and rounded type in group B. The difference was statistically significant in both groups (P<0.05).

Table 1. *Comparisons of the sPAPHA thickness, IAR, and R values between the two groups.*

	group A (n=51)	group B (n=101)	t (χ^2)	p
thickness of sPAPHA (mm)	4.69±2.56	2.86±1.47	6.34	<0.05
IAR (°)	51.42±7.23	59.25±9.37	5.34	<0.05
R	2.89±1.65	2.21±1.02	4.78	<0.05

3.4. Relationship Between Pleural Adhesions and Rough Pleural Surface of Spontaneous Pneumothorax

The spontaneous pneumothorax in 37 cases affected the area in 25 cases, and the pleural surface was rough with localized lengths extending into the lung in a total of 74 cases, including 10 cases of 1 place, 4 cases of 2 places, 4 cases of 3 places, 1 case of 4 places, 2 cases of 5 places, 2 cases of 7 places, and 2 cases of 8 places.

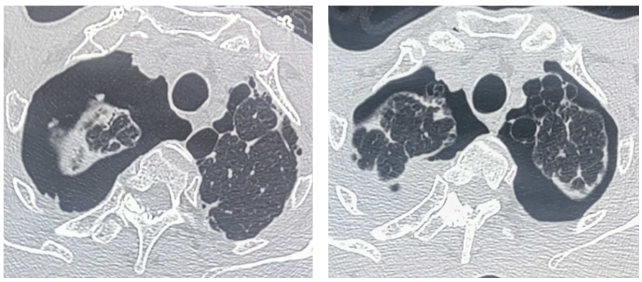

(1) (2)

Figure 9. *(1) and (2) is same patient. Male, 69 years old, spontaneous pneuthorax Re-examination of spontaneous pneumothorax on the right side showed that pneumothorax occurred again on the left side. The three ribs before the upper lung cross section of pneumothorax were rough with high-density strip shadow under the pleura. No adhesion was observed after pneumothorax (white arrow). Two mediastinal pleural surface rough with subpleural high-density strip shadow, adhesion after pneumothorax (black arrow).*

7 cases were found to have striated or membranous adhesions, with an incidence of 9.45% (7/74).

4. Discussion

4.1. Medical Imaging of sPAPHA and PAC

PAC is the accompanying shadows of the first and second ribs in the full chest radiograph dimension; from the bottom up, there are composite images of the pulmonary epithelium, visceral pleura, subpleural cavity, parietal pleura, extrapleural fat, intrathoracic fascia, and the extracostal periosteum. When the thickness of PAC is greater than 5mmn, it is abnormal [3-5]. PAC microscopic pathology only refers to some old fibrous scar tissue in the pulmonary apex, due to relative hypoxia and chronic inflammatory irritation of apex pulmonis, the local pleura is more or less hypertrophic and adhered, and the general pathology is close to the imaging PAC performance. Due to the presence of some fat outside the pleura, the PAC thickness measured by the full chest radiograph is greater than the pathology of real mankind. The sPAPHA, especially the mild sPAPHA, basically reflects the true thickness of PAC, because the parietal pleura is only 0.1 m thick and the visceral pleura is seamlessly connected to the elastic fibers on the lung surface [4-5].

4.2. The Relationship Between sPAPHA and PPFE

The diagnosis of sPAPHA is commonly reported, even among the young population (aged 18 to 40 years). In our research, the discovery rate of sPAPHA was 2.27%, among which 33.55% had radio-PPPE symptoms. The IAR, R value and depressed cupula pleurae ratio in group A were significantly greater than those in group B, which had the characteristics of flat chest and were consistent with the literature [1, 6]. The relevant literature suggested that PAC and PPFE might be manifestations of lesions at different periods and could evolve with each other [7-9]. We assume that radio-PPFE is closely related to PPFE. Due to the IAR of flat chest is large, the depth of thoracic cavity is high and the negative pressure at the apex of the lung is large, the horizontal vector pressure of the respiratory cycle is difficult to release and is transmitted longitudinally, resulting in apical hypertension; depressed cupula pleurae of flat chest causes increased pleural friction coefficient and pulmonary pleural

hypertrophy [10-11]; the apex of lung is in a relatively "anemic" state, because of the restrictive ventilation, compressed small arteries and reduced blood flow, which leads to a series of inflammatory reactions caused by ischemia and hypoxia, resulting in fibrosis and elastic tissue hyperplasia. The IAR of depressed apex of lung is small and the amplitude of thoracic respiratory motion is decreased, which also leads to some degree of restrictive ventilation. In this study, patients in group A had similar imaging findings with sPAPHA pathologically confirmed in the literature [7-8, 12], so it is speculated that they may have a similar pathological basis, mainly as follows: cell-free lamellar mesh basket collagen fibers are tightly attached to the elastic fibers under the mesothelial cells to form a glassy plaque in the visceral pleura. Peculiar triangular plaques along the subpleural lung parenchyma showed distinctive acidity to scarring from superficial to deep, with sparse parenchymal cells and residual dilated fine bronchial walls with small lymph nodes and air spaces with carbon or stone end phagocytosis of macrophages. The fibrotic areas were mainly composed of a wavy bifollicular dense collagen fibrous network, and elastic fiber staining showed that these collagen cords were the original elastic fiber network in the atrophied lung. Thrombus was seen in the small pulmonary arteries, and the venous walls were sclerotic.

4.3. sPAPHA and Pleural Hypertrophy

Pleural adhesions refer to the adhesion between the visceral pleura and the parietal pleura. The existence of adhesions cannot be confirmed in the non-pneumothorax state, but can only be visualized in the pneumothorax state, and the presence of adhesions can be presumed by dynamic imaging with limited slippage of the two pleural layers while subpleural calcification and fibrous strips are only auxiliary signs [13-14]. In this study, only 9.46% of the 37 patients with spontaneous pneumothorax had pleural cavity adhesions at the rough pleural surface with striae shadow. Therefore, strictly speaking, it is not reasonable to diagnose sPAPHA, but it may be more objective to diagnose PAPHA. The diagnosis of early mild pulmonary pleural fibroelastic tissue hyperplasia may be more reasonable for group A patients, who were advised to focus on respiratory function exercises, which would be beneficial in delaying the progression of the disease.

4.4. Differential Diagnosis

PAC, usually old scars, is mostly seen in middle-aged and elderly people. This lesion has non-pleural apical circumferential development, whose pathology is often accompanied by fibroblastic foci; subpleural nodular are seen on imaging, and few of the patients has flat chests. On the other hand, PPFE can be seen in young people, and primary spontaneous pneumothorax is not uncommon in young adults [5]. The youngest patient is 16 years old [15]. PPFE develops circumferentially around the apex of lung, and the pathology shows elastic fibrous tissue hyperplasia, with subpleural thickening of the inverted triangular lobular septa predominating, and the patients have flat chests.

In connective tissue-associated interstitial lung lesions, radio-PPFE can be either PPFE or PAC, and PAC can also be pre-PPFE, which can be difficult to distinguish at certain times in the course of the disease or even pathologically. Immunohistochemistry for myofibroblast flat-footed positive-potoplanin helps to differentiate [9].

4.5. Conclusion

In conclusion direct signs of pleural adhesions cannot be observed in the non-pneumothorax state, and the symmetrical and extensive pleural hypertrophy with multiple subpleural triangular conical solid shadows in both upper lungs may belong to PPFE or pre-PPFE, and the diagnosis of PAPHA may be appropriate for mild and limited cases, while the diagnosis of PAPHA may be appropriate for severe and extensive cases in elderly people and PPEE in young people.

References

[1] ZHU XIAODONG, CAO HETAO, SU HAIBING. et al. Analysis of the Chest Imaging Features of Primary Spontaneous Pneumothorax with Multi-Slice CT Scan [J]. Journal of Clinical Radiology, 2017, 36 (9): 1248-1252.

[2] ODA T, OGURA T, KITAMURA H, et al. Distinct characteristics of pleuroparenchymal fibroelastosis with usual interstitial pneumonia compared with idiopathic pulmonary fibrosis [J]. Chest, 2014, 146: 1248-1255.

[3] ZHANG JICHUN, GU KE. Measurement of normal apex pulmonis companion shadow on the chest film [J]. Shanghai Medical Imaging, 2005, 14 (3): 213-214.

[4] ENOMOTO Y, NAKAMURA Y, COLBY T V, et al. Radiologic pleuroparenchymal fibroelastosis like lesion in connective tissue disease-related interstitial lung disease [J]. PLoS One, 2017, 12 (6) e0180283.

[5] LIANG C, SHUANG L, WEI L, et al. Correlative anatomy of the pleura and pleural spaces [J]. ThoracSurg Clin, 2011, 21: 177–182.

[6] HARADA T, YOSHIDA Y, KITASATO Y, et al. The thoracic cage becomes flattened in the progression of pleuroparenchymal fibroelastosis [J]. Eur Respir Rev, 2014, 23: 263-266.

[7] ESTEVES C, COSTAF R, REDONDO T, et al. Pleuroparenchymal fibroelastosis: role of high-resolution computed tomography (HRCT) and CT-guided transthoracic core lung biopsy [J]. Insights Imaging, 2016, 7 (1): 155–162.

[8] ENOMOTO Y, MATSUSHIMA S, MEGURO S, et al. Podoplanin-positive myofibroblasts: a pathologic hallmark of pleuroparenchymal fibroelastosis [J]. Histopathology, 2018, 72 (7): 1209-1215.

[9] HIRAMI Y, NAKATA M, MAEDA, et al. Pulmonary apical mass, the so-called pulmonary apical cap, in a 43-year-old woman [J]. Ann Thorac Cardiovasc Surg, 2010, 16: 122-124.

[10] CASHA A R, MANCHÉ A, GATT R, et al. Is there a biomechanical cause for spontaneous pneumothorax [J]? European Journal of Cardio-Thoracic Surgery, 2014, 45 (6): 1011–1016.

[11] CAO HETAO, WANG SUJUAN, ZHANG YANMAN, et al. Manifestation of CT Virtual Endoscopy Images of Pleural Cavity [J]. Journal of Clinical Radiology, 2019, 38 (10): 1842-1846.

[12] KOBAYASHI N S, NAMBU A, KAWAMOTO M, et al. Pulmonary apical opacities on thin-section computed tomography: relationship to primary spontaneous pneumothorax in young male patients and corresponding histopathologic findings [J]. J Comput Assist Tomogr, 2018, 42 (1): 33-38.

[13] FELLER-KOPMAN D, LIGHT R. Pleural Disease [J]. N Engl J Med, 2018; 378: 740-51.

[14] WU YONG, ZHU DONG-SHAN, YAO YUN-MING, et al. The study of preoperative detection of pleural adhesions by chest ultrasonogrphy [J]. Chinese Journal of Thoracic and Cardiovascular Surgery. 2010, 26 (3): 190-192.

[15] ATAG E, BAS IKIZOGLU N, GOKDEMIR Y, et al. An adolescent with idiopathic pleuroparenchymal fibroelastosis, Case report [J]. Arch Argent Pediatr, 2018, 116 (1): e147-e150.